Quantitative imaging outperforms No-reflow in predicting functional outcomes in a translational stroke model

Justine Debatisse, Lucie Chalet, Omer Faruk Eker, Tae-Hee Cho, Guillaume Becker, Océane Wateau, Marlène Wiart, Nicolas Costes, Inés Mérida, Christelle Léon, et al.

Neurotherapeutics xxx (xxxx) xxx

Contents lists available at ScienceDirect

Neurotherapeutics

journal homepage: www.sciencedirect.com/journal/neurotherapeutics

Original Article

Quantitative imaging outperforms No-reflow in predicting functional outcomes in a translational stroke model

Justine Debatisse [a,1], Lucie Chalet [a,b,1], Omer Faruk Eker [c,d], Tae-Hee Cho [a,d,e], Guillaume Becker [a], Océane Wateau [f], Marlène Wiart [a], Nicolas Costes [g], Inés Mérida [g], Christelle Léon [a], Jean-Baptiste Langlois [g], Sophie Lancelot [g,h], François Lux [i], Timothé Boutelier [b], Norbert Nighoghossian [a,d,e], Laura Mechtouff [a,d,e], Emmanuelle Canet-Soulas [a,*]

[a] Université Claude Bernard Lyon1, CarMeN Laboratory, INSERM, INRAE, Bât. B13, Groupement Hospitalier Est, 59 Boulevard Pinel, Lyon, France
[b] Olea Medical, La Ciotat, France
[c] Université Claude Bernard Lyon1, CREATIS, CNRS, INSERM, INSA Lyon, Bât. Blaise Pascal, 7 Avenue Jean Capelle, Villeurbanne 69621, France
[d] Neuroradiology Department, Hospices Civils of Lyon, 69000, Lyon, France
[e] Stroke Department, Hospices Civils of Lyon, 69000, Lyon, France
[f] Cynbiose SAS, Marcy-L'Etoile, France
[g] CERMEP - Imagerie du Vivant, Lyon, France
[h] Department of Radiopharmacy, Hospices Civils of Lyon, 69000, Lyon, France
[i] Universite Claude Bernard Lyon1, Institut Lumière Matière, CNRS, France

ARTICLE INFO

Keywords:
Acute ischemic stroke
Thrombectomy
No-reflow
PET-MRI
Blood-brain barrier
Oxygen metabolism

ABSTRACT

Microvascular dysfunction and no-reflow are considered a major cause of secondary damage despite revascularization in acute ischemic stroke (AIS), ultimately affecting patient outcomes. We used quantitative PET-MRI imaging to characterize early microvascular damages in a preclinical non-human primate model mimicking endovascular mechanical thrombectomy (EVT). During occlusion, PET perfusion and MRI diffusion were used to measure ischemic and lesion core volumes respectively. Following revascularization, multiparametric PET-MRI included perfusion, diffusion, blood-brain barrier (BBB) permeability MRI, and ^{15}O-oxygen metabolism PET. Lesion growth on MRI was evaluated at one week, and the neurological score was assessed daily; a poor outcome was defined as a score>6 (0-normal, 60-death) after one week. Early after recanalization, the gold-standard PET ischemic threshold (<0.2 mL/min/g) identified post-EVT hypoperfusion in 67 % of the cases (14/21) located in the occlusion acute lesion. Acquired 110 min post-EVT, the area of MRI *Tmax* hypoperfusion was larger and even more frequent (18/20) and was also located within the acute lesion. Eight of the total cases (38 %) had a poor outcome, and all of them had no-reflow (7/8 MRI no-reflow and 6/8 PET no-reflow). Diffusion *ADC* alterations and post-EVT oxygen extraction fraction (*OEF)* values were significantly different in PET no-reflow cases compared to those without no-reflow, exhibiting an inverse correlation. Independently of no-reflow, long perfusion *Tmax* and post-EVT high BBB *Ktrans* in the lesion core were the hallmarks of poor outcome and infarct growth. This early quantitative imaging signature may predict infarct growth and poor outcome and help to identify neuroprotection targets.

Introduction

In the management of patients with acute ischemic stroke (AIS), intravenous thrombolysis and endovascular mechanical thrombectomy (EVT) have proven their efficacy in improving functional outcomes [1]. However, despite successful recanalization, up to 50 % of patients remain disabled [2]. This futile recanalization can potentially be attributed to ischemia-reperfusion injuries [3,4]. The occurrence of microvascular damages and the subsequent no-reflow appear as direct consequences of endothelial activation and immune cell interaction during ischemia and early post-recanalization periods. The aforementioned phenomenon is intricately linked to thrombotic pathways as well as instability of

* Corresponding author.
E-mail address: emmanuelle.canet-soulas@univ-lyon1.fr (E. Canet-Soulas).
[1] These authors contribute equally.

https://doi.org/10.1016/j.neurot.2025.e00529
Received 6 August 2024; Received in revised form 3 January 2025; Accepted 14 January 2025

hemodynamics, blood shear stress, and cerebrovascular autoregulation during acute phases [5]. Although no-reflow appears as a major factor in ischemia-reperfusion injury in preclinical stroke research [6–9] and in acute myocardial ischemia [10], its impact on the outcome in AIS patients is still a matter of debate and its clinical prevalence has only recently been confirmed in a large cohort of patients after mechanical thrombectomy [11,12].

The no-reflow is characterized by a high degree of variability, and clinical outcomes may not be consistent across all no-reflow cases [13, 14]. Additionally, a discrepancy exists between clinical and pre-clinical data, mainly rodent studies, hindering an in-depth understanding of this microvascular impairment to identify potential therapeutic targets [15]. The modified thrombolysis in cerebral infarction (mTICI) grade is the clinical standard used to evaluate recanalization in patients with AIS. Recent studies showed that reperfusion assessed by perfusion imaging better predicts good outcomes than recanalization using mTICI scores [13,14]. However, readouts following recanalization to predict poor outcomes have not yet been established [15]. The definition of the post-EVT hypoperfused volume is also subject to significant variation based on the imaging modality, i.e. PET, CT, or MRI, as well as the post-processing software used [11,14–16].

This retrospective study aims to evaluate the dynamic features of microvascular damages in a non-human primate (NHP) model mimicking thrombectomy. We developed a sophisticated model of ischemia-reperfusion in NHP with extensive PET-MRI characterization [17]. We used standard stroke MRI protocols associated with quantitative PET cerebral blood flow (*CBF*) and gold standard cerebral metabolic rate of oxygen ($CMRO_2$), as well as quantitative blood-brain barrier (BBB) permeability MRI with two contrast agents of different molecular weights [18]. Preceding analysis uncovered that ciclosporin A (CsA), a potent protector against reperfusion injury, was able to decrease early BBB damage [19] and limit late inflammation [20]. Here, we further analyzed PET-MRI parameters during the critical early stages of AIS to investigate the relationship between microvascular damages and subsequent evolution and assess their possible relation to the functional outcome.

Material and Methods

Experimental design

The animal model and the experimental protocol described previously [19], followed the European guidelines for pre-clinical stroke studies. The trial was approved by the authorities (registration numbers APAFIS#4702 and #8901). Middle cerebral artery occlusion (MCAo) was induced in 7-year-old mature male *Macaca fascicularis* for 110 min by an endovascular coil under sevoflurane anesthesia and continuous monitoring. PET-MRI imaging was performed during occlusion, after coil and thrombus retrieval (post-EVT-like), and after one week (Fig. 1 for study design). Neuro-scores were monitored daily for one month (0 = normal to 60 = death) as described by Debatisse et al. [17]. A persistent score above 6 after one week was considered a poor outcome.

The inclusion criterion was successful occlusion and the exclusion criteria were no revascularization and missing or poor data quality from post-EVT perfusion imaging. The no-reflow was assessed from the decision tree in Fig. 1A using the gold standard PET hypoperfusion threshold (CBF<0.20 mL/min/g) and the Time-to-maximum (*Tmax* > 2sec) MRI previously established in this model at the occlusion phase [17]. Treatment was randomized after inclusion, and analysis was performed blindly at all time points. Ciclosporin A (iv injection 5 min prior to recanalization, 2 mg/kg, Sandimmun®, Novartis) was used as a potential neuroprotective treatment, and saline injection was used as a placebo [19].

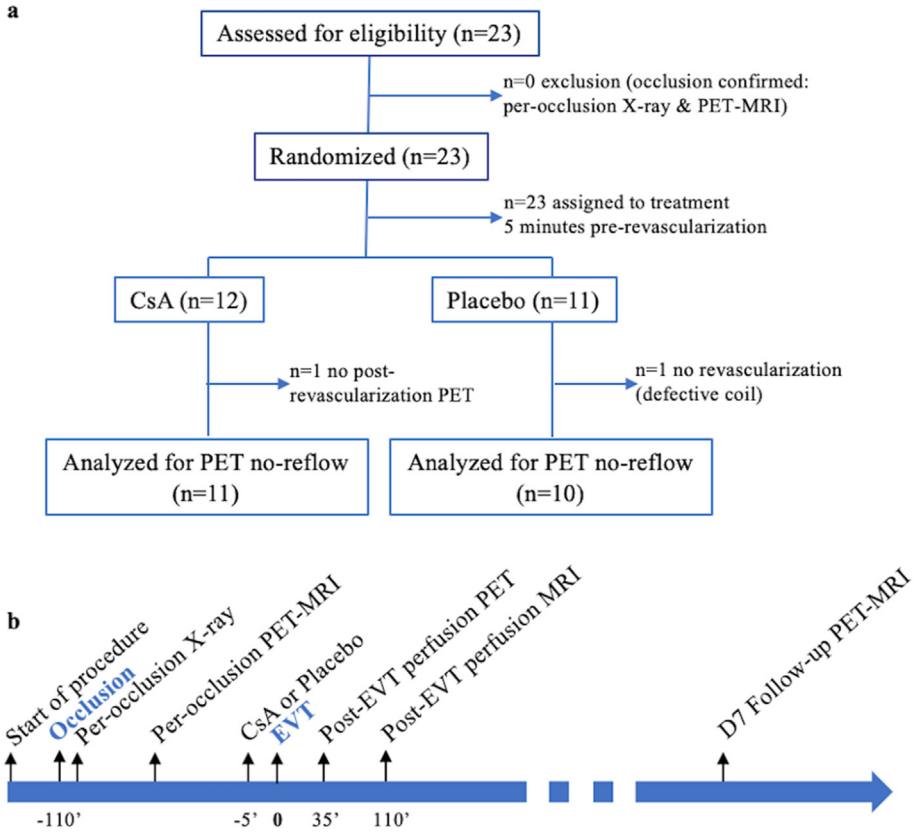

Fig. 1. Flow chart and longitudinal PET-MRI imaging follow-up of the preclinical study (a-b). CsA = ciclosporin A; EVT = endovascular mechanical thrombectomy; MRI = magnetic resonance imaging; PET = positron emission tomography.

PET-MRI protocol

The PET-MRI protocol is summarized in Fig. 1B and was described previously [19]. MRI with standard clinical AIS management sequences was acquired at occlusion, 2 h after revascularization, and at day 7. MRI perfusion-weighted imaging was obtained and analyzed as previously described (Supplemental method) to obtain *Tmax* maps. [^{15}O]H_2O PET was used to quantify perfusion and quantitatively measure the hypoperfused areas at occlusion (ischemic volume) and immediately after revascularization (post-EVT hypoperfused volume) [21–24]. CBF images were obtained from modeling of [^{15}O]H_2O PET, using a one-tissue compartment to compute quantitative CBF maps. In addition, [^{15}O]O_2 was used to measure the cerebral metabolic rate of oxygen ($CMRO_2$) and oxygen extraction fraction (*OEF*) immediately after revascularization, as previously established using bolus inhalation [25] (Supplemental).

High-resolution T1-weighted MPRAGE images were acquired and used to calculate the transformation matrix and non-linear warping was applied to co-register all imaging data on a common space using the *Macaca fascicularis* 3D template [20,26].

Imaging variables

Thresholds of critical hypoperfusion were established at *CBF*<0.2 mL/min/g for PET and *Tmax*>2 s for MRI [17]. Hypoperfused volumes were measured during occlusion and post-recanalization. The post-EVT hypoperfused volumes measured in PET and MRI using the same respective thresholds characterized the no-reflow PET and MRI areas.

Acute lesion core at occlusion and after revascularization and established infarct at day 7 were measured by an experienced stroke neurologist blinded to all preclinical data from diffusion-weighted imaging (DWI) and fluid-attenuated inversion recovery (FLAIR) T2 respectively (Supplemental). Lesion core and hypoperfused (ischemic) volumes were measured in the native space before registration using occlusion data. Penumbra (ischemic tissue not in the core) and lesion growth (FLAIR positive tissue not initially DWI positive) volumes were determined by voxel-based analysis after warping on the *Macaca fascicularis* 3D template space [17]. The DWI core volume was used as the lesion mask to evaluate the quantitative parameters before and after recanalization.

Recanalization was evaluated using MR time-of-flight (TOF) angiography after coil retrieval. It was further confirmed using post-recanalization dynamic susceptibility contrast subtraction analysis to evaluate vascular filling (early, mid, late) [27].

Hemorrhage was evaluated on T2*-weighted imaging as the presence of hypo-intense sub-regions, and graded according to the clinical Heidelberg Classification [28] with HI1 corresponding to small petechiae with no mass effect. BBB damage was visually evaluated by enhancement on post-gadolinium FLAIR and 3D T1 and quantified by dynamic contrast-enhanced (DCE) MRI as previously described [19] using both small Gd-DOTA and larger gadolinium nanoparticles (AGuIX®) (Supplemental) and the same clinical DCE *Ktrans* method. Quantitative values of perfusion, ADC, permeability, and oxygen consumption are obtained after registration and warping on the atlas template space. The mean of voxel's values inside the lesion mask is used for all parameters except for *Ktrans* and *Tmax*, where the median is selected due to a non-gaussian distribution of values. Data are expressed as absolute values as previously described [18].

Statistical analysis

Data were analyzed using GraphPad Prism (9.4.1 version, GraphPad Software, LLC, San Diego, USA). Continuous variables are expressed as means (standard deviation, ±SD) or medians with lower and upper quartiles ([Quartile 1-Quartile 3]) depending on their distributions, and categorical variables as percentages. Means were compared with the Student parametric *t*-test and medians using the Mann–Whitney test for independent samples and the Wilcoxon test for paired comparisons. Normality was evaluated using the D'Agostino and Pearson test. Correlations between continuous variables were tested using the Spearman rank test. Logistic regression evaluated quantitative parameters toward poor outcome prediction. The post-hoc evaluation of identified parameters' prognostic value was done by the receiver operator characteristic (ROC) curve. The area under the curve (AUC) was given with 95 % confidence interval. Tests were two-sided and $p < 0.05$ was considered significant.

Results

Twenty-three animals were included and imaged during occlusion, with a mean DWI lesion core of 4.1 ± 3.2 mL (12 % of the 35 mL hemisphere). They received either ciclosporin A (CsA; n = 12) or saline (n = 11) 5 min before coil retrieval. The post-EVT perfusion PET was acquired 35 [30–40] minutes after revascularization and post-EVT perfusion MRI 110 [105–120] minutes after revascularization. For post-EVT perfusion analysis, one animal was excluded because of the absence of revascularization due to a defective coil, and another animal did not have perfusion PET after recanalization due to a radiosynthesis issue (Fig. 1A). Table 1 summarizes results in the two groups and Supplemental Tables 1–2 display individual results per group. No differences were observed between the CsA and placebo groups in relation to the considered parameters.

Table 1
Characteristics of the Ciclosporin A and Placebo groups.

	CsA (n = 11)	Placebo (n = 10)	p
Age, years	7 [6,7]	7 [6.75–7]	>0.99
BW, kg	8.5 [7–9.6]	7.25 [6.85–9.22]	0.14
M2 MCA segment occlusion side (right/left)	6/5	7/3	
Day 1 neuroscore	21 ± 18	14 ± 11	0.33
SBP at occlusion, mmHg	101 ± 8	99 ± 13	0.11
DBP at occlusion, mmHg	41 ± 7	42 ± 13	0.91
EtCO2 at occlusion, mmHg	32 ± 4	29 ± 4	0.09
Occlusion DWI lesion volume, mL	4 ± 3.5	4.7 ± 2.7	0.62
Occlusion PET CBF ischemic volume, mL	1.2 [0.5–4.1] [a]	3 [2.1–11.1] [b]	0.1
Ischemic penumbra volume, mL	0.9 [0.4–1.6] [a]	1.4 [0.9–9.4] [b]	0.17
Occlusion MRI Tmax ischemic volume, mL	12.5±4.2 [c]	14.6±4.7 [d]	0.35
Post-recanalization DWI volume, mL	4 ± 3.6	3.7 ± 2.9	0.85
Presence of PET no-reflow	7/11	7/10	
PET CBF no-reflow volume, mL	0.7 [0.5–6.1]	0.4 [0.1–5.4]	0.46
PET CBF value in no-reflow area, mL/min/g	0.2 [0.1–0.2]	0.2 [0.2–0.2]	0.9
Presence of MRI no-reflow	11/11	6/9 [$]	
MRI Tmax no-reflow volume, mL	5.2 [1.7–11.9]	11.8 [9.7–15] [$]	0.15
Day 7 FLAIR lesion volume, mL	1.6 [0.5–5.9] [e]	2 [0.4–4.2] [f]	0.89
Infarct growth, mL	0.5[0.3–1.6] [e]	0.7 [0.1–1.5] [f]	0.97
Hemorrhage (HI1)	5/11	4/10	
Day 7 neuroscore	2.5 [0.8–7.3] [e]	5 [0–8] [f]	0.82
Poor outcome	3/11	5/10	0.39

BW = body weight; CsA = ciclosporin A; CBF = cerebral blood flow; DBP = diastolic blood pressure; DWI = diffusion-weighted imaging; FLAIR = fluid-attenuated inversion recovery; SBP = systolic blood pressure.

[a] n = 10 (1 missing PET).
[b] n = 8 (2 missing PET).
[c] n = 10 (1 missing MRI, artifact).
[d] n = 8 (2 missing MRI, artifact); n = 9 (1 missing MRI, artifact).
[e] n = 10 (1 premature death).
[f] n = 9 (1 premature death).

PET and MRI no-reflow volumes

All cases presented successful revascularization evidenced by MR angiography TOF. In the post-revascularization PET analysis (acquired 35 min post-EVT), 14 out of 21 (67 %) of the animals had areas of hypoperfusion, the larger hypoperfused areas occurring in animals with large ischemic volumes at occlusion (median post-EVT hypoperfused PET volume of 0.7 mL [0.2–5.6], n = 14) (Fig. 2a and Supplemental Tables 1–2 for individual results). Overall, 90 % of the animals (18/20) exhibited hypoperfusion from MRI conducted 110 min after recanalization. The estimated hypoperfusion volume was larger using the MRI *Tmax* threshold (>2 s) (7.9 [3.3–15] mL, n = 18) compared to the PET *CBF* threshold (0.7 [0.2–5.6] mL, n = 14, p = 0.0018) (Fig. 2b and Supplemental Tables 1–2). All poor outcome cases (8/21) had either PET or MRI hypoperfusion (Supplemental Tables 1–2). Two poor outcome cases without initial PET no-reflow had large MRI no-reflow (Fig. 2c–d), BBB damage, and persistent no-reflow at day 7. There were small hemorrhagic petechiae in 9/21 cases (43 %), all of them being PET or MRI no-reflow cases (with premature death for two of them and poor outcomes for four) (Table 1 and Supplemental Tables 1–2). Alternatively, 9/13 good outcome cases had either PET or MRI no-reflow.

Multiparametric quantitative PET-MRI and clinical outcome

Using multiparametric quantitative PET-MRI in the DWI core region, the only parameters that significantly differed between PET no-reflow cases (n = 14) and those without no-reflow (n = 7) were ADC at occlusion and post-EVT (p = 0.036 and 0.005, respectively), post-EVT CBF (p = 0.02) and post-EVT OEF (p = 0.02) (Supplemental Table 3). MRI showed a limited number of cases without no-reflow (n = 3) compared to those with no-reflow (n = 15), and only post-EVT ADC was significantly different (p = 0.027). We next focused on multiparametric quantitative PET-MRI and clinical outcome, and evaluated whether poor outcome cases could be distinguished from those with good outcomes in the 21 NHPs.

In cases with poor outcomes, occlusion and post-revascularization *Tmax* were significantly longer than in good outcome cases (p = 0.0018 and 0.019 for occlusion and post-EVT, respectively) (Fig. 3a–b). *CBF* values (p = 0.53 and 0.064 for occlusion and post-EVT, respectively) or other MRI perfusion parameters (regional blood flow or volume, *rBF* or *rBV*, or mean transit time, *MTT*) were not different except for post-EVT *rBV* (for occlusion and post-EVT respectively: *rBF* p = 0.54 and 0.31, *rBV* p = 0.15 and 0.037, *MTT* p = 0.13 and 0.57) (Supplemental Fig. 1 for longitudinal MRI perfusion maps). After revascularization, poor outcome cases tend to have a compromised oxygen metabolism ($CMRO_2$ is decreased despite high *OEF*), though not reaching significance. We next examined BBB damage with DCE *Ktrans* after revascularization. *Ktrans* values in the no-reflow region were correlated to those in the lesion core for both small and larger contrast agents (for Gd-DOTA, r = 0.78, p = 0.0025 and AGuIX, r = 0.76, p = 0.0055 respectively) (Supplemental Fig. 2a and b). *Ktrans* with both contrast agents is significantly higher in poor outcome cases than in good outcome cases (Fig. 3c–d and Fig. 4). Fig. 4 illustrates the multiparametric features in good and poor outcome cases. The poor outcome signature included severe ischemia with long *Tmax* above the threshold at occlusion and still severely altered after recanalization, presence of small petechial hemorrhagic transformation at the time of occlusion, impaired $CMRO_2$ in the same area, and BBB damage (Fig. 4 and Supplemental Fig. 3).

We next evaluated the predictive value of these parameters toward a poor outcome. First, we confirm that infarct growth (voxel-based evaluation) correctly predicts poor outcome (AUC: 0.86; sensitivity: 67 %, specificity: 85 %). We found that, among early quantitative parameters, occlusion *Tmax* and post-EVT Gd *Ktrans* showed similar high predictive value (Fig. 5a–b). Correlation analysis demonstrated the interdependence of the evaluated parameters (Fig. 5c). It confirmed the link between *Tmax* (occlusion and post-EVT), Gd *Ktrans,* and infarct growth. It highlighted the relationship between the post-EVT low $CMRO_2$ and the low *CBF* or long *Tmax*, as well as between low *ADC* values (occlusion and post-EVT) and high *OEF* (Fig. 5d–e, Supplemental Fig. 3).

Discussion

We used quantitative PET-MRI to investigate the dynamic nature of microvascular damage in a pre-clinical stroke model mimicking mechanical thrombectomy. There was post-EVT PET-MRI hypoperfusion in over 50 % of cases, with 50 % poor outcomes in these cases. Low *ADC* values at occlusion correlated with post-EVT high *OEF* and characterized no-reflow cases. In this NHP model, severe occlusion and post-EVT alterations, such as lengthy *Tmax* and increased *Ktrans*, are the best indicators to uncover cases with detrimental consequences, infarct growth, and poor outcomes.

In acute ischemic stroke, the clinical standard to assess recanalization status is the mTICI grade. It paralleled the TIMI score in acute myocardial ischemia, but the clinical assessment of no-reflow strikingly differs between these two pathologies. The myocardial no-reflow corresponds to hypointense sub-regions within the established contrast-enhanced infarct area at one week on late gadolinium contrast-enhanced MRI [10], or its early assessment is done using the index of microvascular resistance at the end of the percutaneous coronary intervention [29]. Myocardial no-reflow is common and is associated with a poor outcome and a higher risk of heart failure independently of the infarct size [29]. The protection of the myocardial microcirculation early after revascularization is therefore a therapeutic target but is still an unmet clinical need. In clinical stroke, the reported incidence of no-reflow is highly variable but can be as high as 57 %, the etiologies are still unclear, and the dynamics of the no-reflow area over time are far from being fully characterized [15,30,31]. In this study, we found hemorrhage (HI1) in half of the no-reflow cases and the endothelial damage was characterized by increased permeability: *Ktrans* was three times higher in poor compared to good outcome cases. Abnormal flow kinetics signed by long MRI *Tmax* at occlusion and 110 min post-EVT, BBB damage characterized by higher *Ktrans*, were the hallmarks of poor prognosis in our model.

Under the ischemia-reperfusion disturbed flow condition, interaction between the activated endothelium and circulating blood cells including neutrophils results in flow stagnation that seems to peak 2–3 h after recanalization in both core and penumbra [9]. These effects may persist for a while in the core region, along with permanent capillary constriction due to pericyte death [6]. Results on our NHP pre-clinical model demonstrated that the no-reflow or “low-reflow” (longer *Tmax*) area was located within the lesion core on the MRI conducted 2 h after recanalization. Consistent with prior observations in the core and penumbra during occlusion, we also found that oxygen metabolism was characterized by an increased *OEF* and a relatively preserved $CMRO_2$ after revascularization. *CBF*, *OEF,* and $CMRO_2$ are highly influenced by both systemic and local blood hemodynamics, as well as arterial levels of O_2/CO_2 with cerebrovascular autoregulation. This balance is known to be compromised and varies over time during the acute phases of ischemic stroke, however, further research is required to investigate this matter thoroughly [32]. We provide evidence that NHPs with poor outcomes exhibit a more significant increase in *Tmax* values at occlusion and after revascularization in the lesion core. It has been emphasized recently that *Tmax* values could be more valuable than using the established threshold to define hypoperfusion [16,33,34]. Indeed, we found that neither *CBF* nor MRI blood flow or blood volume were different in poor outcome cases. Further investigation is required to determine the etiologies of no-reflow, which may be attributed to various factors including poor collaterals inducing fast progression of cytotoxic edema, hemodynamic instability (important variations in systolic blood pressure, oxygen saturation or $EtCO_2$), early microvascular damage inducing metabolic disruption, hemorrhage, or inflammation [15].

Furthermore, it is proposed that *OEF* and $CMRO_2$ may serve as additional viable metrics for assessing the efficacy of neuroprotective

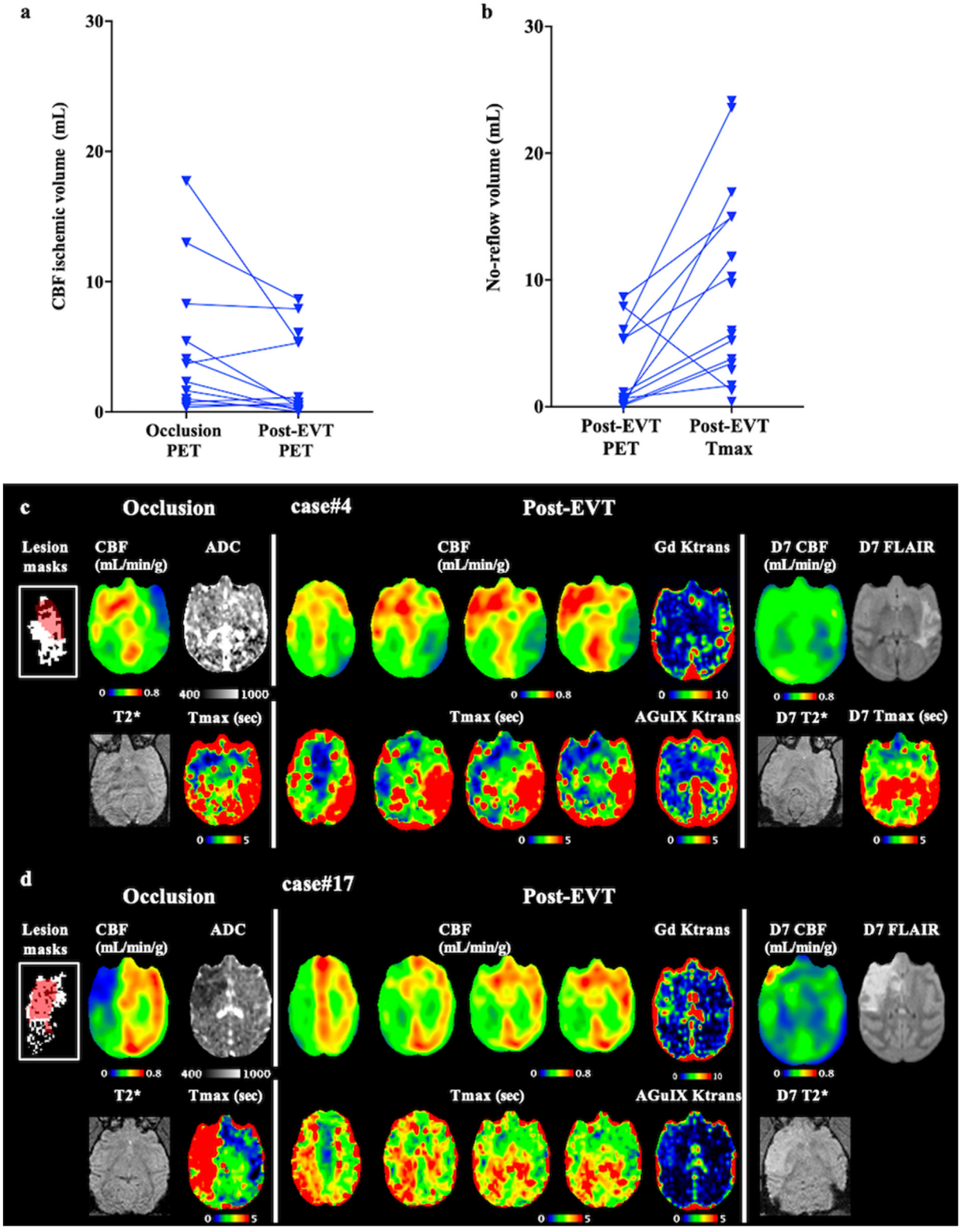

Fig. 2. PET no-reflow volumes after revascularization (post-EVT) compared to their corresponding ischemic volumes at occlusion. (**a**). Post-revascularization (post-EVT) no-reflow areas were larger with MRI *Tmax* acquired 75 min after their respective PET (**b**). Two examples without initial PET *CBF* no-reflow where MRI *Tmax* map identifies large no-reflow (4 slices) resulting in poor outcome (**c-d**). Boxes (left) represent the lesion masks defined at occlusion (DWI core, white and PET ischemia, red overlay). Case#4 (initial and day 7 neuroscores:18–8) had large MRI no-reflow with blood-brain barrier (BBB) damage (high transfer rate *Ktrans*) for both small gadolinium (Gd, 0.5 kDa) and nanoparticles (AGuIX, 10 kDa) contrast agents (**c**); case #17 (initial and day 7 neuroscores: 18–60, coma and death after imaging) had large MRI no-reflow, with BBB damage (high *Ktrans* for the small Gd contrast agent) (**d**) and persistent no-reflow at day 7 (deconvolution for *Tmax* mapping failed due to abnormally slow kinetics).

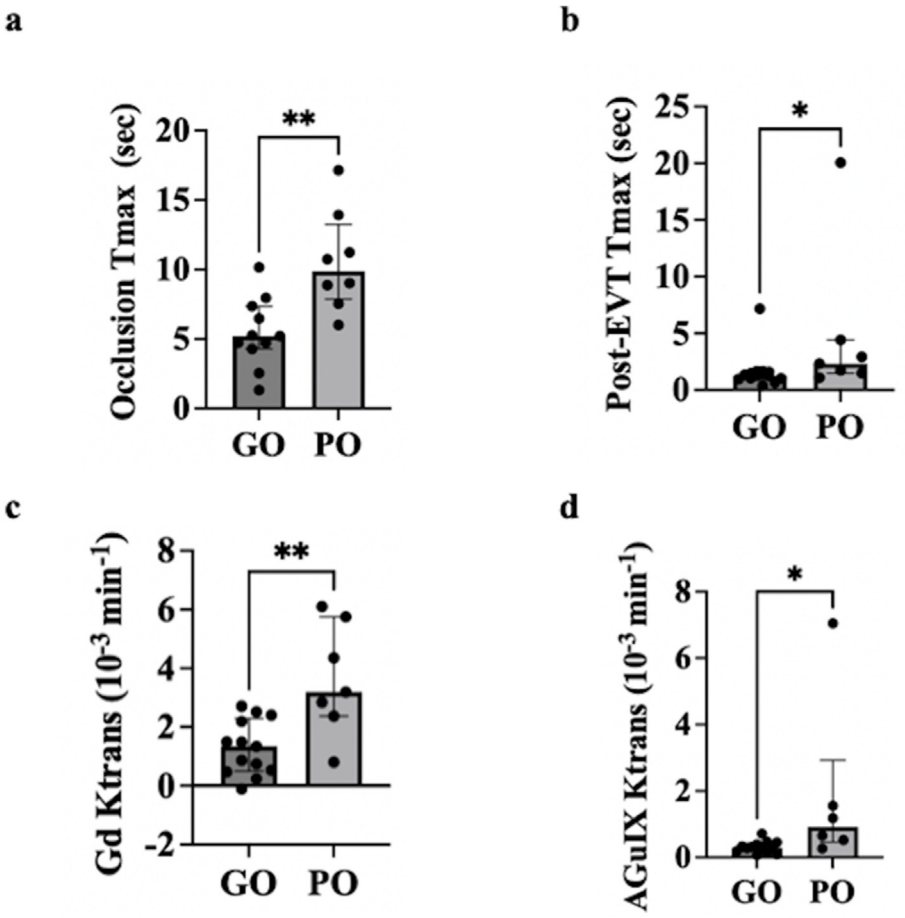

Fig. 3. Occlusion and post-revascularization (post-EVT) multiparametric quantification in poor outcome (PO) and good outcome (GO) in the DWI lesion core. At occlusion (**a**) and post-EVT (**b**), MRI *Tmax* were significantly longer in PO compared to GO. Blood-brain barrier damage measured by transfer rate *Ktrans* is significantly more pronounced in PO using both small gadolinium (Gd) and large (AGuIX nanoparticles) contrast agents (**c, d**).

interventions during the acute phase combined with diffusion measurements [35]. The relationship between low *ADC* values from the occlusion time and increased *OEF* together with reduced *CBF* (Fig. 5) after revascularization should be confirmed by further studies and mechanistic approaches [6]. One limitation is that PET $CMRO_2$ is no longer possible in clinical stroke studies [23,36] due to radioprotection regulations. Validation of MRI *OEF* and $CMRO_2$ using the blood oxygenation level-dependent (BOLD) effect as a substitute is necessary in the post-revascularization scenario [37]. Future studies may also use MRI $OEF/CMRO_2$ imaging to predict motor/cognitive deficits during the chronic phases after stroke.

One important consideration for future clinical study design is the timing to start the protection of the microcirculation. Our study showed that no-reflow damage and its related poor outcome may have early determinants during the occlusion time, as evidenced by the long *Tmax* and low *ADC* value correlating with the post-EVT no-reflow BBB leakage and altered oxygen metabolism. From these findings, we could infer that microcirculation protection should start as soon as possible, even during the occlusion period as evidenced in recent and ongoing studies of neuroprotection against excitotoxicity (the ESCAPE-NEXT and the ongoing FRONTIER trials): the earlier the better, and possibly in the golden hour of ischemic stroke [38].

As with any model, we acknowledge certain limitations. The occlusion is induced by a thrombogenic coil, which may exhibit differences from the thromboembolic conditions observed in patients. In addition, the evaluation of recanalization was assessed using the MR angiography TOF sequence after coil retrieval, rather than the gold-standard digital subtraction angiography and the mTICI score. The no-reflow phenomenon was assessed using quantitative perfusion measurement, which indeed corresponds to the current recommendations for myocardial ischemia-reperfusion [10]. Up to now, Ng et al. recommended to use of MRI or CT *rBF* or *rBV* in acute ischemic stroke [12] but post-EVT perfusion imaging is still rarely performed and usually at 24 h or later [15]. In our hand, *Tmax* at occlusion and post-EVT was the most robust MRI perfusion parameter, compared to the other parameters (Supplemental Fig. 1). In a recent retrospective clinical study [39], long Tmax (>10s) was found to be the best predictor of fast early infarct growth, which aligns with our findings. Furthermore, this marker was suggested for patient eligibility to new treatment targeting fast progression. Tmax may not reflect only microvascular flow. As very recently exposed by Yedavalli et al. [40], the venous outflow can be evaluated on Tmax maps in specific venous regions. In this article, patients with poor venous outflow also had larger areas with Tmax values > 10s in the lesion.

We also acknowledge that we were not able to find a protective effect of CsA on clinical outcomes despite its pleiotropic targeting of the no-reflow features (BBB, mitochondria, inflammation). This is certainly due to the small sample size as the retrospective power calculation indicated that a sample size of 40–50 per group would have been necessary given the variability in lesion core and infarct size. However, it is difficult to perform larger study groups in NHP research for obvious ethical reasons.

In conclusion, we found early no-reflow in a preclinical model mimicking EVT evolving during the first 2 h after successful revascularization. The prevalence and magnitude of the observed phenomenon were greater when evaluated through MRI *Tmax* as opposed to PET *CBF*. We further evaluated perfusion, edema, BBB damage, and oxygen

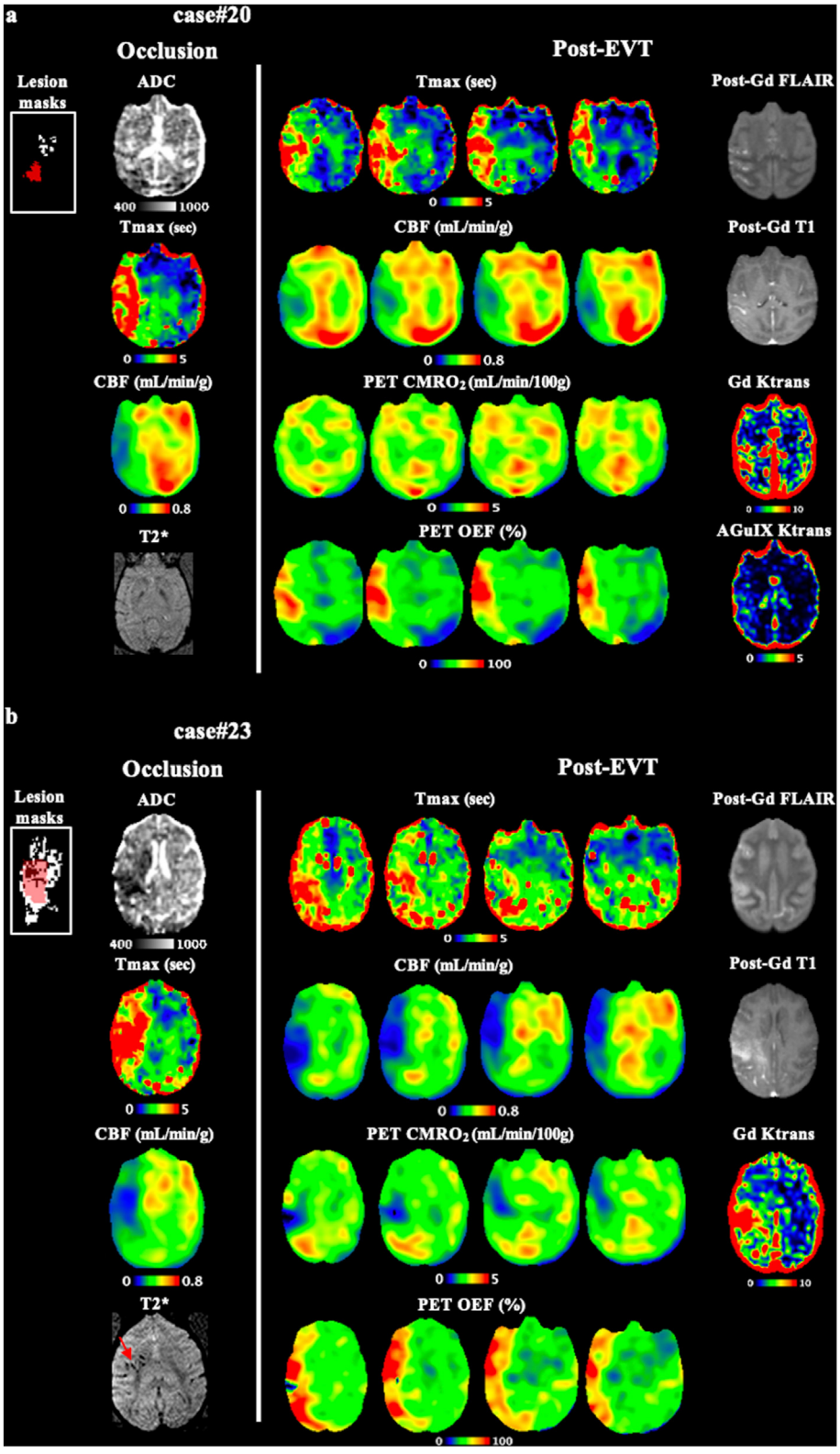

Fig. 4. Multiparametric maps at occlusion and post-revascularization as differential readouts of no-reflow cases. Post-EVT maps (4 slices) of two no-reflow cases (**a-b**). The white boxes (left column) represent the masks defined at occlusion, respectively DWI lesion core (white) and PET ischemia (red overlay). Both cases had large no-reflow areas on MRI *Tmax* (**a-b**, first line). Case#20 (initial neuroscore = 3; day 7 neuroscore = 0) showed a post-EVT preserved oxygen consumption ($CMRO_2$) and high oxygen extraction fraction (*OEF*) (**a**), whereas case#23 (initial neuroscore = 33; deceased at D1) showed profound post-recanalization perfusion (*CBF* PET) and $CMRO_2$ defect and large area of suffering tissue (high *OEF*) (**b**). These features were associated with small hemorrhagic petechiae on T2* already present at occlusion (arrow) and marked blood-brain barrier damage (post-gadolinium enhancement on FLAIR and T1, and transfer rate *Ktrans* maps with high *Ktrans* values). *Ktrans* with the larger AGuIX contrast agent was not available for case#23.

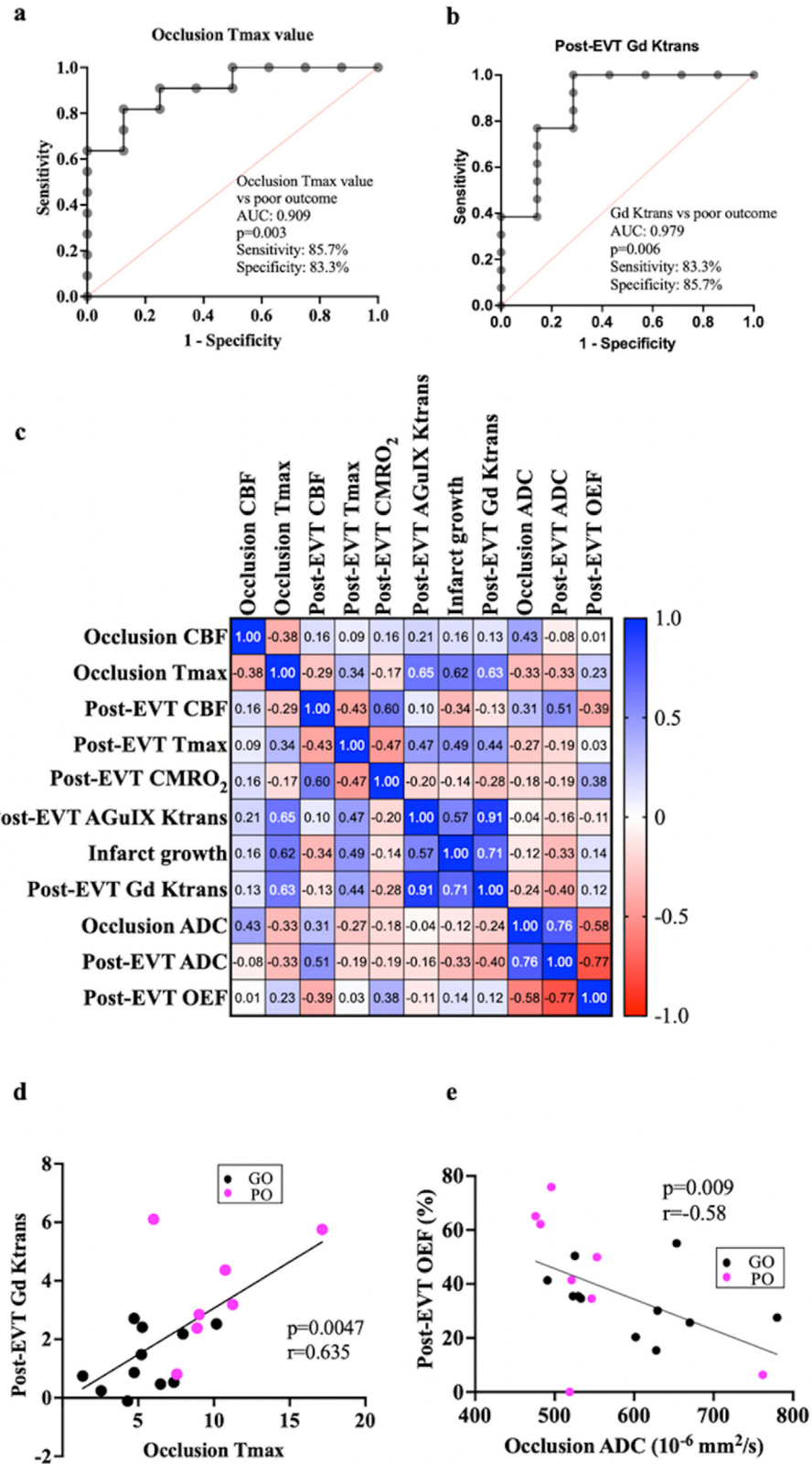

Fig. 5. Predictive values of parameters and their interrelationship at occlusion and after revascularization. Occlusion *Tmax* value in the lesion core had a good ability to predict poor outcome (AUC: 0.9, sensitivity: 86 %, specificity: 83 %) (**a**) as well as the post-revascularization (post-EVT) permeability measurement *Ktrans* using large nanoparticles AGuIX (AUC: 0.98, sensitivity: 83 %, specificity: 86 %) (**b**). Correlation analysis demonstrated the interrelationship of the evaluated parameters (**c**) and confirmed the link between *Tmax* (occlusion and post-EVT), *Ktrans,* and infarct growth. Post-EVT, the Gd *Ktrans* is correlated to the perfusion *Tmax* measured during occlusion (**d**), and the oxygen extraction fraction (*OEF*) is inversely correlated to the apparent diffusion coefficient (*ADC*) measured during occlusion (**e**). Poor outcome (PO) cases are in magenta and good outcome (GO) cases are in black.

metabolism and found that quantitative parameters in the lesion core better predict infarct growth and poor outcome than no-reflow. In future studies, they may be used to monitor early treatment effects and predict futile recanalization.

Authors Contribution (according to Contributor Role Taxonomy (CRediT)

Conceptualization: ECS, JD, OFE, THC, NN, LM.
Data curation: JD, ECS, NC, IM.
Formal analysis: JD, ECS, THC, LM, LC.
Funding acquisition: NN, THC, ECS.
Investigation: JD, OEF, THC, OW, NC, IM, CL, JBL, DLB, SL.
Methodology: JD, ECS, NC, IM, DLB, LC, MW, GB, FL.
Project administration: ECS.
Resources: ECS, JD, OFE, OW, FL.
Software: JD, NC, IM, TB, LC.
Supervision: ECS, JD, OFE, THC.
Validation: ECS, JD, NN, THC, LM.
Visualization: JD, ECS, OFE, THC, LM, NN.
Writing – original draft: JD, ECS.
Writing – review & editing: All authors.

Funding

This work was supported by ANR CYCLOPS and CMRO2 (ANR-15-CE17-0020 and ANR-21-CE17-0028), the RHU MARVELOUS (ANR-16-RHUS-0009) of Lyon University, under the Investissements d'Avenir program of the French National Research Agency (ANR). The PET–MRI acquisitions were carried out thanks to the Equipex LILI funding (LIL-I—Lyon Integrated Life Imaging: hybrid MR-PET ANR-11-EQPX-0026). The PhD salary of L.C. (Cifre, OLEA Medical) is co-funded by the French Ministry of Higher Education and Research (ANRT).

Disclosure

Lucie Chalet and Timothe Boutelier are employees of Olea Medical. The authors have declared that no competing interest exists.

Ethical approval

All applicable international, national, and/or institutional guidelines for the care and use of animals were followed.

This article does not contain any studies with human participants performed by any of the authors.

Declaration of competing interest

The authors declare the following financial interests/personal relationships which may be considered as potential competing interests: Canet Soulas reports financial support was provided by French National Research Agency. Lucie Chalet reports a relationship with Olea Medical that includes: employment. Timothe Boutelier reports a relationship with Olea Medical that includes: employment. If there are other authors, they declare that they have no known competing financial interests or personal relationships that could have appeared to influence the work reported in this paper.

Acknowledgment

This work was supported by ANR CYCLOPS and CMRO2 (ANR-15-CE17-0020 and ANR-21-CE17-0028), the RHU MARVELOUS (ANR-16-RHUS-0009) of Lyon University, under the Investissements d'Avenir program of the French National Research Agency (ANR). The PET–MRI acquisitions were carried out thanks to the Equipex LILI funding (LIL-I—Lyon Integrated Life Imaging: hybrid MR-PET ANR-11-EQPX-0026). The PhD salary of L.C. (Cifre, OLEA Medical) is co-funded by the French Ministry of Higher Education and Research (ANRT).

Appendix A. Supplementary data

Supplementary data to this article can be found online at https://doi.org/10.1016/j.neurot.2025.e00529.

References

[1] Powers WJ, Rabinstein AA, Ackerson T, Adeoye OM, Bambakidis NC, Becker K, et al. Guidelines for the early management of patients with acute ischemic stroke: 2019 update to the 2018 guidelines for the early management of acute ischemic stroke: a guideline for healthcare professionals from the American heart association/American stroke association. Stroke [Internet] 2019 [cited 2022 Aug 31];50:344-418, https://www.ahajournals.org/doi/10.1161/STR.0000000000000211.
[2] Shi ZS, Liebeskind DS, Xiang B, Ge SG, Feng L, Albers GW, et al. Predictors of functional dependence despite successful revascularization in large-vessel occlusion strokes. Stroke 2014;45:1977–84.
[3] Dirnagl U, Iadecola C, Moskowitz MA. Pathobiology of ischaemic stroke: an integrated view. Trends Neurosci 1999;22:391–7.
[4] Bai J, Lyden PD. Revisiting cerebral postischemic reperfusion injury: new insights in understanding reperfusion failure, hemorrhage, and edema. Int J Stroke 2015;10:143–52.
[5] Fan JL, Nogueira RC, Brassard P, Rickards CA, Page M, Nasr N, et al. Integrative physiological assessment of cerebral hemodynamics and metabolism in acute ischemic stroke. J Cerebr Blood Flow Metabol 2022;42:454–70.
[6] Hall CN, Reynell C, Gesslein B, Hamilton NB, Mishra A, Sutherland BA, et al. Capillary pericytes regulate cerebral blood flow in health and disease. Nature 2014;508:55–60.
[7] Yemisci M, Gursoy-Ozdemir Y, Vural A, Can A, Topalkara K, Dalkara T. Pericyte contraction induced by oxidative-nitrative stress impairs capillary reflow despite successful opening of an occluded cerebral artery. Nat Med 2009;15:1031–7.
[8] El Amki M, Glück C, Binder N, Middleham W, Wyss MT, Weiss T, et al. Neutrophils obstructing brain capillaries are a major cause of No-reflow in ischemic stroke. Cell Rep 2020;33:108260.
[9] Erdener ŞE, Tang J, Kılıç K, Postnov D, Giblin JT, Kura S, et al. Dynamic capillary stalls in reperfused ischemic penumbra contribute to injury: a hyperacute role for neutrophils in persistent traffic jams. J Cerebr Blood Flow Metabol 2021;41:236–52.
[10] Kloner RA, King KS, Harrington MG. No-reflow phenomenon in the heart and brain. Am J Physiol Heart Circ Physiol 2018;315:H550–62.
[11] Schiphorst A ter, Charron S, Hassen WB, Provost C, Naggara O, Benzakoun J, et al. Tissue *no-reflow* despite full recanalization following thrombectomy for anterior circulation stroke with proximal occlusion: a clinical study. J Cerebr Blood Flow Metabol 2021;41:253–66.
[12] Ng FC, Churilov L, Yassi N, Kleinig TJ, Thijs V, Wu T, et al. Prevalence and significance of impaired microvascular tissue reperfusion despite macrovascular angiographic reperfusion (No-reflow). Neurology 2022;98:e790–801.
[13] Potreck A, Mutke MA, Weyland CS, Pfaff JAR, Ringleb PA, Mundiyanapurath S, et al. Combined perfusion and permeability imaging reveals different pathophysiologic tissue responses after successful thrombectomy. Transl. Stroke Res 2021;12:799–807.
[14] Carbone F, Busto G, Padroni M, Bernardoni A, Colagrande S, Dallegri F, et al. Radiologic cerebral reperfusion at 24 h predicts good clinical outcome. Transl. Stroke Res 2019;10:178–88.
[15] Sperring CP, Savage WM, Argenziano MG, Leifer VP, Alexander J, Echlov N, et al. No-reflow post-recanalization in acute ischemic stroke: mechanisms, measurements, and molecular markers. Stroke 2023;123:044240. STROKEAHA.
[16] Engedal TS, Hjort N, Hougaard KD, Simonsen CZ, Andersen G, Mikkelsen IK, et al. Transit time homogenization in ischemic stroke – a novel biomarker of penumbral microvascular failure? J Cerebr Blood Flow Metabol 2018;38:2006–20.
[17] Debatisse J, Wateau O, Cho TH, Costes N, Mérida I, Léon C, et al. A non-human primate model of stroke reproducing endovascular thrombectomy and allowing long-term imaging and neurological read-outs. J Cerebr Blood Flow Metabol 2021;41:745–60.
[18] Zaro-Weber O, Fleischer H, Reiblich L, Schuster A, Moeller-Hartmann W, Heiss W. Penumbra detection in acute stroke with perfusion magnetic resonance imaging: validation with ^{15}O-positron emission tomography. Ann Neurol 2019;85:875–86.
[19] Debatisse J, Eker OF, Wateau O, Cho TH, Wiart M, Ramonet D, et al. PET-MRI nanoparticles imaging of blood–brain barrier damage and modulation after stroke reperfusion. Brain Communications 2020;2:fcaa193.
[20] Becker G, Debatisse J, Rivière M, Crola Da Silva C, Beaudoin-Gobert M, Eker O, et al. Spatio-temporal characterization of brain inflammation in a non-human primate stroke model mimicking endovascular thrombectomy. Neurotherapeutics 2023;20:789–802.
[21] Zaro-Weber O, Moeller-Hartmann W, Siegmund D, Kandziora A, Schuster A, Heiss WD, et al. MRI-based mismatch detection in acute ischemic stroke: optimal PWI maps and thresholds validated with PET. J Cerebr Blood Flow Metabol 2017;37:3176–83.
[22] Baron J, Moustafa RR. Perfusion thresholds in cerebral ischemia. In: The ischemic penumbra; 2007. p. 21–35.

[23] Heiss WD, Zaro Weber O. Validation of MRI determination of the penumbra by PET measurements in ischemic stroke. J Nucl Med 2017;58:187–93.
[24] Reimer J, Montag C, Schuster A, Moeller-Hartmann W, Sobesky J, Heiss WD, et al. Is perfusion MRI without deconvolution reliable for mismatch detection in acute stroke? Validation with ^{15}O-positron emission tomography. Cerebrovasc Dis 2018;46:16–23.
[25] Kudomi N, Hayashi T, Teramoto N, Watabe H, Kawachi N, Ohta Y, et al. Rapid quantitative measurement of CMRO $_2$ and CBF by dual administration of ^{15} O-Labeled oxygen and water during a single PET scan—a validation study and error analysis in anesthetized monkeys. J Cerebr Blood Flow Metabol 2005;25:1209–24.
[26] Ballanger B, Tremblay L, Sgambato-Faure V, Beaudoin-Gobert M, Lavenne F, Le Bars D, et al. A multi-atlas based method for automated anatomical Macaca fascicularis brain MRI segmentation and PET kinetic extraction. Neuroimage 2013;77:26–43.
[27] Higashida RT, Furlan AJ. Trial design and reporting standards for intra-arterial cerebral thrombolysis for acute ischemic stroke. Stroke [Internet] 2003;34 [cited 2022 Aug 31], https://www.ahajournals.org/doi/10.1161/01.STR.0000082721.62796.09.
[28] von Kummer R, Broderick JP, Campbell BCV, Demchuk A, Goyal M, Hill MD, et al. The Heidelberg bleeding classification: classification of bleeding events after ischemic stroke and reperfusion therapy. Stroke 2015;46:2981–6.
[29] Carrick D, Haig C, Ahmed N, Carberry J, Yue May VT, McEntegart M, et al. Comparative prognostic utility of indexes of microvascular function alone or in combination in patients with an acute ST-segment–elevation myocardial infarction. Circulation 2016;134:1833–47.
[30] Dalkara T. Pericytes: a novel target to improve success of recanalization therapies. Stroke 2019;50:2985–91.
[31] Horsch AD, Dankbaar JW, Niesten JM, van Seeters T, van der Schaaf IC, van der Graaf Y, et al. Predictors of reperfusion in patients with acute ischemic stroke. AJNR Am J Neuroradiol 2015;36:1056–62.
[32] Nogueira RC, Beishon L, Bor-Seng-Shu E, Panerai RB, Robinson TG. Cerebral autoregulation in ischemic stroke: from pathophysiology to clinical concepts. Brain Sci 2021;11:511.
[33] Gwak DS, Choi W, Kwon JA, Shim DH, Kim YW, Hwang YH. Perfusion profile evaluated by severity-weighted multiple Tmax strata predicts early neurological deterioration in minor stroke with large vessel occlusion. J Cerebr Blood Flow Metabol 2022;42:329–37.
[34] Kishi F, Nakagawa I, Kimura S, Ogawa D, Yagi R, Yamada K, et al. *T* max volume can predict clinical type in patients with acute ischemic stroke. Brain and Behavior 2023;e3163.
[35] Yu Y, Christensen S, Ouyang J, Scalzo F, Liebeskind DS, Lansberg MG, et al. Predicting hypoperfusion lesion and target mismatch in stroke from diffusion-weighted MRI using deep learning. Radiology 2023;307:e220882.
[36] Derdeyn CP, Khosla A, Videen TO, Fritsch SM, Carpenter DL, Grubb RL, et al. Severe hemodynamic impairment and border zone-region infarction. Radiology 2001;220:195–201.
[37] Eker OF, Ameli R, Makris N, Jurkovic T, Montigon O, Barbier EL, et al. MRI assessment of oxygen metabolism and hemodynamic status in symptomatic intracranial atherosclerotic stenosis: a pilot study. J Neuroimaging 2019;jon:12615.
[38] Fisher M, Savitz SI. Pharmacological brain cytoprotection in acute ischaemic stroke — renewed hope in the reperfusion era. Nat Rev Neurol 2022;18:193–202.
[39] Seners P, Yuen N, Olivot JM, Mlynash M, Heit JJ, Christensen S, et al. Factors associated with fast early infarct growth in patients with acute ischemic stroke with a large vessel occlusion. Neurology 2023;101(21):e2126–37.
[40] Yedavalli VS, Koneru M, Hoseinyazdi M, Greene C, Lakhani DA, Xu R, et al. Prolonged venous transit on perfusion imaging is associated with higher odds of mortality in successfully reperfused patients with large vessel occlusion stroke. J NeuroIntervent Surg 2024. jnis-2024-021488.